

# Population pharmacokinetics of enfuvirtide in pediatric patients with human immunodeficiency virus: Searching for exposure-response relationships

**Objective:** Our objective was to describe the population pharmacokinetics and pharmacodynamics of enfuvirtide acting on viral ribonucleic acid in children with human immunodeficiency virus 1.

**Methods:** A 1-compartment population pharmacokinetic model with first-order absorption and elimination was fit to subcutaneous and intravenous dose pharmacokinetic data from a 2-part study, as follows: an intensive-sample pharmacokinetic design (observed dose) (subcutaneous and intravenous,  $n = 12$ ) followed by a sparse-sample design (unobserved dose) (subcutaneous,  $n = 15$ ). The parameters of this model are clearance (CL), volume of distribution (V), absorption rate ( $k_a$ ), bioavailability (F), and both interindividual and residual variability. Plasma ribonucleic acid concentrations over time were used to build a population viral pharmacodynamics model with the following parameters: viral clearance ( $CL_v$ ), initial viral concentration ( $A_0$ ), duration ( $\tau$ ) and rate (R) of preinfected cell-based viral input after enfuvirtide was begun, and interindividual and residual variability.

**Results:** The mean population CL and V of enfuvirtide for a child with a mean body weight of 21.3 kg were 1.42 L/h and 5.67 L, respectively. Patient weight affected CL and V. Volume appeared to differ between intensive and sparse sampling occasions, and this difference also affected the residual error variance. Time after the beginning of therapy did not significantly affect any pharmacokinetic parameter, supporting the absence of metabolic induction and inhibition. Although trends were present, no statistically significant relationship was seen between any pharmacokinetic-based individual enfuvirtide exposure measure and any virologic response measure.

**Conclusions:** Regarding pharmacokinetics and pharmacodynamics, no statistically significant correlation between exposure measures and viral clearance was observed. (Clin Pharmacol Ther 2003;74:569-80.)

**Dolors Soy, PhD, Francesca T. Aweeka, PharmD, Joseph A. Church, MD, Coleen K. Cunningham, MD, Paul Palumbo, MD, Bradley W. Kosel, PharmD, Lewis B. Sheiner, MD, and the Pediatric AIDS Clinical Trial Group (PACTG) Study P1005**

**Investigators** San Francisco and Los Angeles, Calif, Syracuse, NY, Newark, NJ, and Seattle, Wash

The use of combination therapy (highly active anti-retroviral therapy) for the treatment of patients with

human immunodeficiency virus (HIV) has been associated with decreased morbidity and mortality rates and

From the Department of Biopharmaceutical Sciences and Department of Clinical Pharmacy, School of Pharmacy, and Department of Laboratory Medicine, School of Medicine, University of California-San Francisco, San Francisco; Division of Clinical Immunology and Allergy, Department of Pediatrics, Childrens Hospital Los Angeles and Keck School of Medicine, University of Southern California, Los Angeles; Pediatric Infectious Diseases, State University of New York, Upstate Medical University, Syracuse; Division of Allergy/Immunology/Infectious and Pulmonary Diseases, Department of Pediatrics, New Jersey Medical School, Newark; and University of Washington, Harborview Medical Center, Seattle.

This work was supported in part by Hoffmann-La Roche Inc, Nutley, NJ, and the Pediatric AIDS Clinical Trials Group, National Institute of Allergy and Infectious Diseases and National Institute of

Child Health and Human Development, National Institutes of Health. Dr Soy was supported by a research grant from Hospital Clínic Barcelona (Pharmacy Service), Barcelona, Spain.

Presented in part at the Fortieth Annual Meeting of the Infectious Diseases Society of America, Chicago, Ill, October 24-27, 2002 (poster No. 441).

Received for publication March 31, 2003; accepted Sept 5, 2003.

Reprint requests: Lewis B. Sheiner, MD, Box 0626, University of California-San Francisco, San Francisco, CA 94143-0626.

E-mail: lbs@c255.ucsf.edu

Copyright © 2003 by the American Society for Clinical Pharmacology & Therapeutics.

0009-9236/2003/\$30.00 + 0

doi:10.1016/j.cpt.2003.09.002

improved quality of life for both adult and pediatric populations.<sup>1-4</sup> A continued high rate of treatment failure, resulting from either the emergence of drug-resistant viruses or an intolerance to drug regimens, motivates a continued search for new drugs with different mechanisms of action and toxicity profiles.<sup>5</sup>

Enfuvirtide (Fuzeon; Trimeris, Inc, Durham, NC; Hoffmann-La Roche Inc, Nutley, NJ) is a member of a new class of antiretroviral drugs, fusion inhibitors,<sup>6</sup> which are small peptides that inhibit the fusion of the viral and target cell membranes.<sup>7,8</sup> Enfuvirtide is a peptide mimetic (36 amino acids) of a region of gp41,<sup>9,10</sup> which has shown its efficacy and safety in patients with HIV that is resistant to current treatments.<sup>11-13</sup>

Church et al<sup>14</sup> reported that in 14 children (aged 4-12 years) with plasma human immunodeficiency virus 1 (HIV-1) ribonucleic acid (RNA) concentrations equal to or exceeding 10,000 copies/mL despite combination antiretroviral therapy the addition of a subcutaneous (SC) dose of enfuvirtide (30 mg/m<sup>2</sup> [n = 4] or 60 mg/m<sup>2</sup> [n = 10]) to the treatment regimen every 12 hours resulted in significant HIV RNA decline. By day 7 after treatment was started, 78% of children in that study reached the protocol target of 0.7 log reduction in HIV RNA from baseline. This decline persisted up to week 24 of treatment in 71% of patients. No severe side effects were observed.

After intravenous (IV) administration, Kilby et al<sup>15</sup> found volumes of distribution (V) ranging between 2.77 and 8.80 L and total clearance (CL) values between 1.5 and 2.7 L/h (mean, 2.02 L/h) after a wide range of drug doses (3-100 mg). They saw no evidence of nonlinear kinetics. Linear kinetics has also been reported after SC administration up to doses of 100 mg enfuvirtide.<sup>16,17</sup>

Zhang et al<sup>18</sup> reported a total CL of  $1.44 \pm 0.3$  L/h and V of the central compartment of  $3.8 \pm 0.8$  L and of the peripheral compartment of  $1.7 \pm 0.6$  L for adults.

Few pharmacokinetic (PK) or pharmacodynamic (PD) data have been presented for enfuvirtide in pediatric populations.<sup>14,19</sup> The purpose of this study is to describe the pharmacokinetics of enfuvirtide and exposure-response to this drug in such a population.

## METHODS

**Study design.** The PK-PD data analyzed here were generated as a component of the Pediatric AIDS Clinical Trial Group (PACTG) Study P1005, a 2-part phase 1/2, multicenter, open-label clinical trial of enfuvirtide treatment conducted by the PACTG investigators that enrolled 15 pediatric HIV-infected subjects (12 in part

A and 3 additional subjects in part B). The following inclusion criteria were used: Children had to be receiving stable additional antiretroviral therapy for at least 16 weeks, have plasma HIV RNA levels greater than or equal to 10,000 copies/mL, and have no prior treatment (or very limited such treatment) with either nonnucleoside reverse transcriptase inhibitors or protease inhibitors. An analysis of the safety and antiretroviral activity of the enfuvirtide treatment in these subjects has previously been reported by Church et al.<sup>14</sup>

The research ethics committee at each center participating in the study approved the protocol, and written informed consent was obtained from the legal guardian or parents of each subject.

**Drug formulation.** Enfuvirtide (Trimeris) was supplied as a lyophilized powder. Specific directives for reconstitution in sterile water and for SC administration were given to parents or guardians.

**PK sampling.** Two different PK sampling approaches were used. In part A of the study, 12 subjects, who were continuing to receive their unaltered background antiretroviral therapy, additionally received a single dose of 15 mg/m<sup>2</sup> (n = 4), 30 mg/m<sup>2</sup> (n = 4), or 60 mg/m<sup>2</sup> (n = 4) enfuvirtide subcutaneously, as well as another such dose, intravenously, on a separate occasion at least 1 day later. Intensive blood sampling was performed after each enfuvirtide dose at 0, 0.5, 1, 2, 4, 6, 8, and 12 hours after dose administration. The primary objective of part A was to identify the SC dose for part B that would likely result in a minimum 12-hour enfuvirtide concentration exceeding 1000 ng/mL, the expected effective concentration based on preclinical data.<sup>15,17,20</sup>

In part B of the study, 14 subjects (11 patients from part A plus 3 additional patients [see later]) were studied as follows. Randomly timed enfuvirtide concentrations (most of which, as was subsequently determined, were drawn just before a dose was administered) were measured on days 1, 3, 7, and 10 and at weeks 4, 16, 24, and 48 (1 measurement per occasion on multiple occasions) of the 30 mg/m<sup>2</sup> every 12 hours or 60 mg/m<sup>2</sup> every 12 hours SC outpatient dose regimen. The background antiretroviral treatment was maintained in all of the part B patients for at least the first 7 days of enfuvirtide treatment. On day 7, while enfuvirtide was continued, each subject's background regimen was changed to include new antiretroviral agents, with at least 1 from an antiretroviral class to which the subject had limited or no prior exposure. Also on day 7, enfuvirtide dose magnitude was increased from 30 mg/m<sup>2</sup> to 60 mg/m<sup>2</sup> in subjects who had not attained 0.7 log 10

plasma HIV-1 RNA decline or in whom trough drug concentrations were lower than 1000 ng/mL on day 7.<sup>21</sup>

Eleven patients participated in both parts of the study; 1 part A patient declined to participate in part B, and 3 patients who had not participated in part A were enrolled in part B. The time (mean  $\pm$  SD) between parts A and B was  $3.6 \pm 2.9$  months (range, 1-10 months).

All data from both PK study designs were merged into a single data set, the analysis of which is the subject of this report.

**Enfuvirtide concentrations.** For PK analysis, blood was collected in heparinized tubes; the plasma was separated, frozen at  $-20^{\circ}\text{C}$ , and shipped within a few days to Trimeris for analysis by use of a no-wash sandwich immunoassay with electrochemiluminescence detection. In brief, plasma samples were incubated with a murine antienfuvirtide monoclonal antibody labeled with ruthenium-tagged *Tris*-bipyridine chelate and a second murine antienfuvirtide monoclonal antibody labeled with biotin. After a 1-hour incubation, immune complexes were captured via streptavidin-coated parametric beads. After addition of buffer and incubation, electrochemiluminescence was measured.

The lower limit of quantification of this assay was 5 ng/mL. Quality-control samples were prepared at 7.5, 30, and 120 ng/mL. Interday and intraday coefficients of variation ranged from 2.5% to 11.4% for all standards and quality control samples. Recovery ranged from 99.9% to 108% (Venetta T, written personal communication, Aug 4, 2003).

All analyses were carried out at a single laboratory (Igen International, Inc, Gaithersburg, Md).

**Viral load and CD4.** Blood samples to determine HIV RNA plasma levels and CD4 lymphocyte counts were collected in all but 1 subject (1 of those participating in both parts) over the whole period of study. Plasma HIV RNA samples were scheduled at days 1, 3, 7, 10, and 18 after initiation of long-term enfuvirtide dosing and at weeks 4, 8, 12, 20, 24, 32, 40, and 48 and were measured with a reverse transcriptase-polymerase chain reaction assay (Roche Amplicor HIV Monitor Ultrasensitive; Roche Molecular Systems, Inc, Branchburg, NJ), with a lower limit of quantification of 50 copies/mL, performed at a single division of an acquired immunodeficiency syndrome (AIDS)-certified laboratory. CD4 counts were obtained by certified AIDS Clinical Trials Group laboratories with standard fluorescence-activated cell analysis.

**Population PK model.** A 1-compartment population PK model with first-order elimination and first-order

absorption of SC doses was fit to the data by use of NONMEM software<sup>22</sup> (GloboMax LLC, Hanover, Md) with the first-order conditional estimation method. The population PK parameters of this model are population typical CL, V, absorption rate ( $k_a$ ), and SC bioavailability (F). Interindividual variability in these parameters, including a correlation between CL and V, and residual (within-individual) observation error were both modeled as log-normally distributed. Subsequently, the covariates weight and sex were tried in the model, to explain interindividual variability. Covariates were retained if they were associated with a significantly improved fit. The difference in minus twice the log likelihood—the NONMEM objective function—between a full model (including a covariate) and a reduced model (without the covariate) is asymptotically chi square-distributed with degrees of freedom equal to the difference in number of parameters between the models. Covariates were included in the model if they yielded  $P < .05$  according to this test.

By use of the final model (ie, with all significant covariates included [see “Results” section and Appendix], where the model is given in full mathematic detail), the following maximum a posteriori (MAP) Bayesian estimates of subject-specific interdose interval, steady-state exposure measures (with the assumption that prescribed prior dosage was taken) were computed for all subjects: (1) area under the enfuvirtide concentration versus time curve (AUC), (2) time at which the maximum enfuvirtide concentration was expected to occur ( $t_{\max}$ ), (3) expected maximum enfuvirtide concentration ( $C_{\max}$ ), and (4) expected minimum enfuvirtide concentration ( $C_{\min}$ ). One value for each of these PK measures was obtained per occasion. A single value for each exposure metric per patient was computed as the average of all of the individuals’ occasion-specific values.

**Population PD model.** After a time delay, the rate of decrease in plasma RNA levels after treatment was started should reflect the degree of efficacy.<sup>23-27</sup> To accommodate the delay-decay features of viral kinetics, we modeled the viral load as given by the state of a 1-compartment model with fixed unit volume and a subject-specific first-order elimination rate that accounted for the net rate of change of free virus resulting from continued production (despite drug) and elimination. A steady-state infusion of virus at a subject-specific rate, assumed to cease at the time drug administration was begun, established baseline viral RNA. Beginning at that time and ending at a subject-specific time, another viral infusion was given at a subject-specific rate, which represented continuing (zero-order)

**Table I.** Estimates of pharmacokinetic parameters

Parameter	Estimate
$\theta_{CL,1}$ (L/h)	1.30 (0.11)
$\theta_{V,1}$ (L)	5.16 (0.11)
$\theta_{ka,1}$ ( $h^{-1}$ )	0.29 (0.09)
$\theta_{F,1}$	0.91 (0.15)
$\theta_{CL,2}$	0.44 (0.56)
$\theta_{V,3}$	2.03 (0.40)
$\theta_{V,2}$	0.43 (0.44)
$\theta_{SP,3}$	1.03 (0.41)
$\omega_{CL}^2$ (%)	37
$\omega_V^2$ (%)	27
$\omega_{ka}^2$ (%)	21
$\omega_F^2$ (%)	40
$cov_{CL-V}$	0.099
$\sigma^2$ (%)	28

Precision (SE) of estimates is expressed as fraction of estimate (in parentheses).

$\theta_{CL,1}$ , Enfuvirtide clearance for an individual with average weight;  $\theta_{V,1}$ , volume of distribution for nonsparse (part A) data for an individual with average weight;  $\theta_{ka,1}$ , absorption rate;  $\theta_{F,1}$ , subcutaneous bioavailability;  $\theta_{CL,2}$ , power of weight in power function predicting enfuvirtide clearance;  $\theta_{V,3}$ , multiplier of volume of distribution for sparse data;  $\theta_{V,2}$ , power of weight in power function predicting enfuvirtide volume of distribution;  $\theta_{SP,3}$ , multiplier of residual error for sparse data;  $\omega_P^2$ , interindividual pharmacokinetic parameter variance; (P = CL [clearance], V [volume of distribution],  $k_a$  [absorption rate], F [bioavailability]);  $cov_{CL-V}$ , covariance between CL and V;  $\sigma^2$ , residual error variance.

viral production from CD4 cells that were already infected after further infection was stopped or diminished by the beginning of the drug. The population parameters estimated with this model are therefore as follows: clearance of virus ( $CL_v$ ), initial concentration of virus ( $A_{v0}$ ), and length ( $\tau$ ) and rate (R) of viral "infusion" after time 0 from already infected cells. The distribution of individual values of all parameters was assumed to be log-normal, as the (independent) distribution of residual error. The model is given in full mathematic detail in the Appendix.

**Response measures.** The fitted viral dynamic PD model was used to generate subject-specific MAP Bayesian estimates of  $CL_v$  and  $\tau$ , which were used as PD response measures, as described subsequently.

The following additional outcome variables (PD response measures) were computed directly from the PD data: (1) time that average RNA was below baseline ( $TARNA_t$ ), calculated by applying the trapezoidal rule to the RNA data between time 0 and day t; (2) the change in log<sub>10</sub> RNA between baseline and day 7 of treatment, divided by the time difference (7 days) (slope 07); (3)  $\Delta$  log-RNA ( $\Delta RNA_t$ ), the difference in log<sub>10</sub> RNA between the baseline and t = 7 days, t = week 24, and t = week 48; and (4) a categorical variable (viral) failure or success, as defined by the

parent study protocol, which considers success to be a 0.7 log<sub>10</sub> plasma RNA decrease by 7 days after the beginning of therapy.

**Exposure-response.** Scatterplots, linear regression, or logistic regression (for the binary success-failure outcome), as appropriate, were used to assess the relationship between all pairwise combinations of (MAP Bayesian estimates of) exposure measures and PD response measures at day 7 and week 24. In addition, a relationship between exposure measures and viral dynamics was sought by including the former as covariates affecting  $CL_v$ , because this should be the main parameter affected by the drug.

## RESULTS

**Demographics.** The median age of the subjects included in the study was 8.2 years (range, 4.0-12.1 years). Part A recruited 8 girls and 4 boys with a mean weight of 30 kg (range, 12.5-76.2 kg). The 14 part B enrollees included 8 girls and 6 boys with a mean weight of 21.3 kg (range, 12.5-76.2 kg).

**Population PK model.** The final PK model was a 1-compartment model (a 2-compartment model was tested but did not improve the fit) including patient weight as a covariate acting on both CL and V (Table I,  $\theta_{CL,2}$  and  $\theta_{V,2}$ ), as well as an offset for sparse (design B) versus intensive (design A) PK samples, acting on mean V (Table I,  $\theta_{V,3}$ ). A similar offset variable was included in the error model (Table I,  $\theta_{SP,3}$ ), accounting for a difference between the residual SD of the sparse samples' error relative to that of the intensive samples. Estimates of all fixed and random effect parameters of the final PK model are given in Table I.

Notably, the time (after the beginning of therapy) was not a significant covariate for any PK parameter, suggesting the absence of metabolic induction and inhibition.

Fig 1 illustrates some basic goodness-of-fit plots for the model. Individual PK profiles of enfuvirtide during the intensive PK study (part A, 12 individuals) are depicted in Fig 2, which shows PK model predictions for a typical individual, as well as the MAP Bayesian estimate for each individual.

No explanation was found for the inability of the model to fit concentrations early in time after IV administration (this fact accounts for the marked discrepancy between observed and predicted PK at high predicted values in Fig 1) in those children receiving the highest dose per kilogram (Fig 2; individuals 4, 10, and 11).

**Population PD model.** The estimated population PD model parameters are listed in Table II. Interindividual

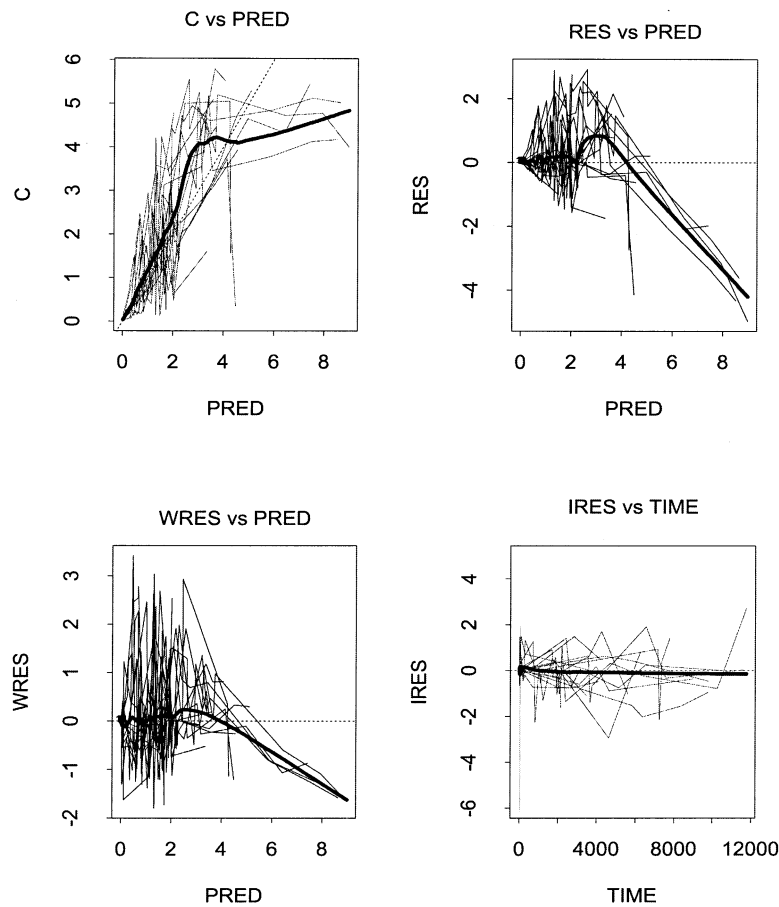


**Fig 1.** Goodness-of-fit plots for population pharmacokinetic (PK) model. *Left upper panel*, Plot of population predictions (PRED) versus observed enfuvirtide concentrations (C) (*dashed line*, line of identity; *thick line*, data smooth). *Right upper panel*, Plot of residuals (RES) versus population predictions (*thick line*, smooth). *Left lower panel*, Plot of weighted population residuals (WRES) versus population predictions (*thick line*, smooth). *Right lower panel*, Plot of individual residuals (IRES) (observed value minus individual prediction) versus time in hours (*thick line*, smooth). Concentrations (C and PRED) are in milligrams per liter; time is in hours.

variability in the rate of loss of preinfected cells could not be estimated. Inclusion of (MAP Bayesian estimates of) enfuvirtide CL (or AUC) as a covariate did not improve the goodness of fit of the PD model.

**Exposure-response.** Individual MAP Bayesian estimates of  $\tau$  and  $CL_v$  are plotted against AUC,  $t_{max}$ ,  $C_{min}$ , and  $C_{max}$  in Fig 3. No significant relationship was seen for any combination of these PK and PD measures. Likewise, no significant relationships were found between AUC and any of the direct data-based PD measures examined:  $TARNA_7$ ,  $\Delta RNA_7$ , slope 07, or  $TARNA_t$  or  $\Delta RNA_t$  for  $t = 24$  weeks or  $t = 48$  weeks. Nor was any statistically significant association found between any PK measure (either at day 7 or at week 24) and failure-success by logistic regression.

## DISCUSSION

Knowledge of both PK and exposure-response is important for optimal dosing. Although many PK-PD studies have been carried out in adults and have yielded updated recommendations and guidelines for HIV treatment, few reports of pediatric PK-PD data are available.<sup>28-30</sup>

This study provides initial information on the PK of enfuvirtide in a group of HIV-1-infected children. The mean population CL (CL/F) and V (V/F) of enfuvirtide obtained in this study for an individual with a body weight of 21.3 kg (which is the average body weight of our subjects) are 1.30 (1.42) L/h and 5.16 (5.67) L, respectively.

Steady-state PK measures such as the area under the curve versus time from 0 to 12 hours [AUC(0-12)] from

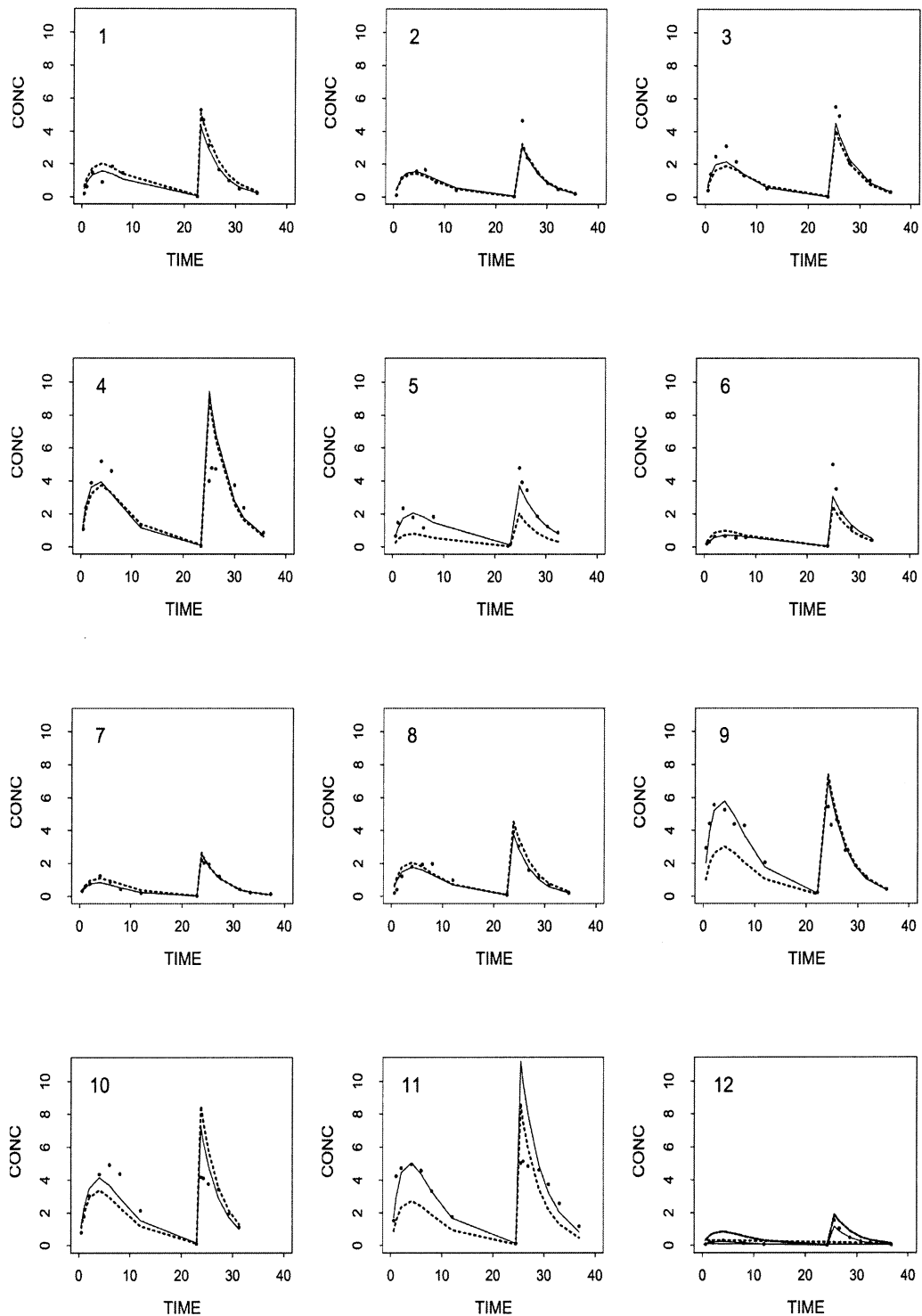


**Fig 2.** Population PK model: Individual maximum a posteriori (MAP) Bayesian enfuvirtide concentration predictions (*solid line*), population (typical individual) predictions (*dashed line*), and observed concentrations (*dots*) for (nonsparse sample) single-dose subcutaneous and intravenous enfuvirtide data only. Enfuvirtide concentrations (CONC) (*ordinate*) are in milligrams per liter; time (*abscissa*) is in hours.

an intensive PK study<sup>19</sup> in children (n = 7) and adolescents (n = 13) who received 1 week of SC therapy with 2 mg/kg enfuvirtide were used to compute and compare CL/F with our results, obtained with a comparable dose (1.8 ± 0.5 mg/kg) and population. Bellibas et al<sup>19</sup> reported trough concentrations of 2.51 ± 1.04 µg/mL and a mean AUC(0-12) value of 49.1 µg · h/mL, which corresponds to a CL/F [Dose/AUC(0-12)] of 0.95 L/h in the studied group of children (mean weight, 23.3 kg; mean age, 8 years). These results are in conflict with those found here (C<sub>min</sub> = 1.80 ± 1.02 µg/mL and CL/F = 1.42 L/h). The main differences between their study and our study concern the PK study design and the PK analysis. In the study by Bellibas et al, PK sampling was intensive over a 12-hour period after dosing at 1 week of enfuvirtide therapy. Parameters were estimated by using standard noncompartmental methods. In this study both intensive and sparse data were taken over a follow-up period of 48 weeks, and a model-based analysis was done. As mentioned previously (see Results section), there is no evidence that length of time on a treatment regimen influences either CL or V, so one might suspect that differences are related primarily to differences in study design (notably, the presence of sparse samples in our study).

In 12 adult subjects who received 90 mg enfuvirtide subcutaneously twice daily for 6 days, Zhang et al<sup>31</sup> found the following values (mean ± SD) for AUC, C<sub>min</sub>, and C<sub>max</sub>, computed by use of model-independent methods: 49 ± 13 µg · h/mL, 2.7 ± 0.8 µg/mL, and 5.7 ± 1.8 µg/mL, respectively. The corresponding values in our pediatric population were lower, as follows: 33.51 ± 17.22 µg · h/mL, 1.80 ± 1.02 µg/mL, and 3.46 ± 1.76 µg/mL, respectively.

The allometric scaling estimated from the pediatric data analyzed here (weight is included in the model as a power function; Fig 4 depicts the functional relationship between CL [V] and weight) predicts (extrapolates) that an individual (adult) with a mean body weight of 70 kg will have a CL (CL/F) and a V (V/F) of 2.16 (2.37) L/h and 6.62 (7.27) L, respectively. A PK study conducted by Kilby et al<sup>15</sup> in a group of adult patients who received IV enfuvirtide twice daily estimated volumes of distribution ranging between 2.77 and 8.80 L and total clearance between 1.5 and 2.7 L/h (mean, 2.02 L/h) after a wide range of drug doses (3-100 mg). These values are similar to our findings. After SC administration of 50 or 100 mg enfuvirtide to adults,<sup>17</sup> steady-state values of CL/F, computed from reported values of AUC(0-12), were 2.34 and 2.74 L/h, respectively, which are also in agreement with the CL/F value (2.37 L/h) we obtained from our pediatric model

**Table II.** Estimates of pharmacodynamic parameters

Parameter	Estimate
A <sub>v0</sub> (HIV-RNA copies/mL)	4.59 (0.23)
τ (d)	1.95 (0.29)
R (HIV RNA copies/mL per day)	4.05 (0.41)
CL <sub>v</sub> (mL/d)	0.44 (0.10)
ω <sup>2</sup> <sub>A<sub>v0</sub></sub> (%)	83
ω <sup>2</sup> <sub>τ</sub> (%)	54
ω <sup>2</sup> <sub>CL<sub>v</sub></sub> (%)	26
σ <sup>2</sup> (%)	16

Estimates of interindividual variability are expressed as coefficients of variation (percent). Precision (SE) of estimates is expressed as fraction of estimate (in parentheses).

A<sub>v0</sub>, Baseline viral RNA; RNA, ribonucleic acid, HIV, human immunodeficiency virus; τ, time of “death” of infected target cell already infected at beginning of therapy; R, rate of “death” of these preinfected cells; CL<sub>v</sub>, clearance of virus; ω<sup>2</sup><sub>P</sub>, interindividual pharmacodynamic parameter variance (P = A<sub>v0</sub>, τ, CL<sub>v</sub>); σ<sup>2</sup>, residual error variance.

after extrapolation to an adult with a mean body weight of 70 kg.

However, our predicted “adult” PK parameters are not compatible with those observed in adults (by use of a 2-compartment model analysis) by Zhang et al.<sup>18</sup> Even after the fact that our data were analyzed according to a 1-compartment model is taken into account (without a prior distribution on the additional parameters, our data do not support a 2-compartment model over a single-compartment model), our predictions exceed their observations (see Fig 4). With the assumption that there is no unknown systematic cause (eg, unobserved covariate) to account for the discrepancy, this reinforces the caution that allometric scaling constants derived from pediatric data, even when those data span a large weight range as here, do not necessarily capture all differences between children and adults. Kovarik et al,<sup>32</sup> for example, reported a reduction in basiliximab clearance in children compared with adults that is independent of age, weight, and body surface area, apparently related to metabolic changes associated with puberty.

The mean enfuvirtide SC F value obtained in the pediatric population (0.91 [91%]) agrees with the values reported for the same route of administration in adults by Zhang et al.<sup>18</sup> As stated by those authors, a “depot” effect can be observed after SC administration of high doses of enfuvirtide. In our study the SC absorption rate constant was close to the elimination rate constant (k<sub>e</sub> = CL/V) (0.25 h<sup>-1</sup>) (Table I), and this could be due to the “depot” effect hypothesized by Zhang et al.

The time between parts A and B was 3.6 ± 2.9 months (mean ± SD) (range, 1-10 months); any car-

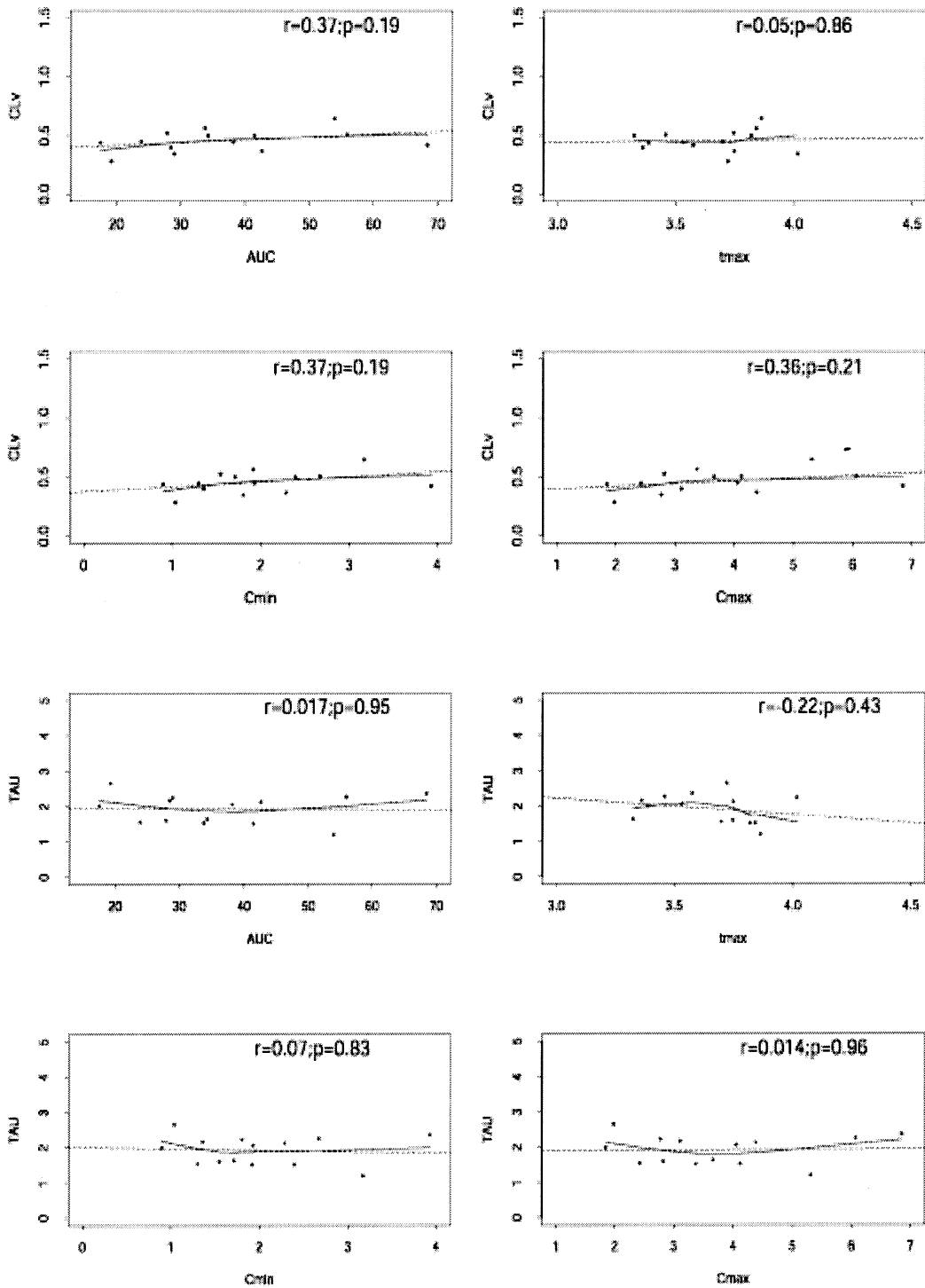


**Fig 3.** Individual estimates of clearance of virus ( $CL_v$ ) and length of time ( $\tau$ ) of continuing viral production by previously infected cells after time 0, plotted against different exposure measures. *Dashed line*, Linear regression; *solid line*, smooth.

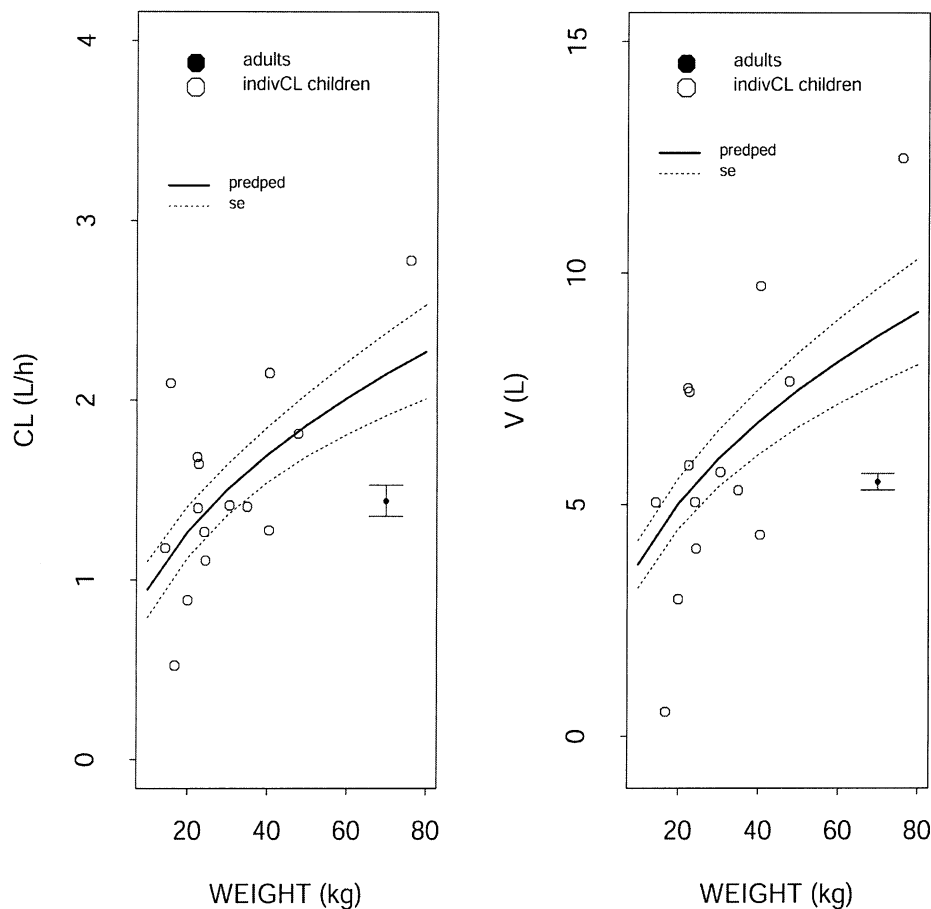


**Fig 4.** PK parameters (*left*, clearance [CL]; *right*, volume of distribution [V]) versus weight. *Open circles*, MAP Bayesian individual predictions of CL and V. *Diamonds*, Mean (*bars*,  $\pm$ SE) from published data in adults (Zhang et al<sup>18</sup>), assuming a mean weight of 68 kg. *Solid lines*, CL and V versus weight for a typical adult individual, as predicted by the PK model developed on pediatric data in this study. *Dashed lines*, SE of predictions (*solid lines*).

ryover effect was thereby avoided, and the viral load was allowed to return to set point.

A “correction” term for sparse (part B) data (trough enfuvirtide concentrations obtained during maintenance therapy) was needed in our PK model as a covariate affecting V to partially explain the interindividual variability related to this PK parameter. It was noticeable that higher values of V were estimated when only 1 concentration per occasion (trough level) was available.

Bearing in mind that the samples in our part B data were collected during long-term therapy at home over a 48-week period, we speculate that problems in compliance (among others) explain the apparent increase in the volume of distribution for part B data (ie, if non-compliance causes lower concentrations than expected

at the nominal dose, it will be associated with a higher estimate of V, which is made by assuming that, possibly contrary to fact, the nominal dose was given).

The lack of trend in the right bottom panel of Fig 1 (individual residuals versus time) suggests that PK parameters do not change over time, and consequently, no metabolic induction or inhibition is taking place over the time course observed in this study.

The reason that the PK model fails to fit IV concentrations early in time for those subjects to whom a large dose per weight was given is not clear (Fig 2), but it does not appear to have been a problem with the administration of the infusion, because in only 1 of these subjects, in whom the IV line infiltrated and had to be restarted, was such a problem noted. We re-estimated our model after deleting these data to determine the

sensitivity of our parameter estimates to them. No important changes in either fixed or random effect parameter estimates resulted, increasing our confidence that, despite our inability to fit certain of our IV data well, our parameter estimates probably do apply to future patients.

A decline in HIV RNA (copies per milliliter) was evident in all patients by day 7 of treatment, and it remained low for the rest of the study period for most of them. It was, therefore, reasonable to confine our dynamic PD model to the events of these first 7 days of treatment, allowing it to be much simpler than a model required to describe long-term viral dynamics. Because our PD analysis was limited to the first week of enfuvirtide treatment, before any changes were made in the other antiretroviral treatments, the decay in HIV RNA could be causally linked to the enfuvirtide administration.

As was noted by Church et al,<sup>14</sup> 3 of 15 subjects (20%) did not reach the protocol enfuvirtide concentration target ( $\geq 1000$  ng/mL) by day 7 after treatment was started. All 3 subjects had received a dose of only 30 mg/m<sup>2</sup> enfuvirtide. After the dosage was changed to 60 mg/m<sup>2</sup>, the target was attained in these individuals. This suggests that for most children 60 mg/m<sup>2</sup> enfuvirtide twice daily should be adequate to reach the 1000 ng/mL exposure target. This dosage corresponds (on a per square meter basis) to the recommended adult dose of 90 mg.<sup>11,15,33</sup>

It is both disappointing and perplexing that strong exposure-response relationships were not seen in this analysis. Although the anticipated positive trend between AUC (exposure) and  $\Delta$ RNA (response) could be observed at all time points tested (7 days, week 24, and week 48), no trend achieved statistical significance. A negative relationship was expected between slope 07 and AUC, and this was seen at day 7 but, again, was not statistically significant ( $P = .64$ ). Finally, a positive relationship was expected between AUC and TARN, and such a trend was observed at both week 24 and week 48, but, likewise, neither relationship was statistically significant ( $P = .48$  and  $P = .69$ , respectively). Moreover, this same relationship was weakly negative at day 7, a distinctly counterintuitive result.

The above-mentioned caution notwithstanding, we note in Fig 3 that the relationship between individual estimates of  $CL_v$ , expected to be the first and most directly affected response variable, and several exposure measures (AUC,  $C_{min}$ ,  $C_{max}$ ,  $t_{max}$ ) all went in the "right" direction, although we stress again that they all failed statistical tests for significance.

The possible reasons for the failure to find an exposure-response relationship in these data are as follows: (1) Such a relationship may be present but obscured by variability, given the small number of subjects studied ( $N = 14$ ). (2) The exposure variability was not great, and all exposures may have been supramaximal. (3) It may be masked by the presence of variable unmeasured active metabolites or other substances that interact with the parent drug in the PK-PD relationship. The third explanation is unlikely, however, because metabolic studies have not discovered such substances.<sup>31</sup>

The PACTG Study Team includes Joseph Church, MD, Childrens Hospital Los Angeles, Los Angeles, Calif; Coleen Cunningham, MD, State University of New York (SUNY) Upstate Medical University, Syracuse, NY; Paul Palumbo, MD, New Jersey Medical School, Newark, NJ; Prakash Sista, Trimeris, Inc, Durham, NC; Michael Hughes, PhD, Harvard School of Public Health, Boston, Mass; Elizabeth Smith, MD, Division of Acquired Immunodeficiency Syndrome (DAIDS), National Institute of Allergy and Infectious Diseases (NIAID), Bethesda, Md; Lynne Mofenson, MD, FAAP, Center for Research for Mothers and Children (CRMC), National Institute of Child Health and Human Development (NICHD), Rockville, Md; Elizabeth Hawkins, PACTG Operations, Rockville, Md; Terence Fenton, EdD, Statistical and Data Analysis Center, Brookline, Mass; Pamela Bouquin, BA, and Kathleen Kaiser, BA, Frontier Science and Technology, Buffalo, NY; Nancy Karthas, RN, MS, CPNP, Children's Hospital, Boston, Mass; Lynette Purdue, PharmD, DAIDS, NIAID, Bethesda, Md; William Shearer, MD, PhD, Texas Children's Hospital, Houston, Tex; Francesca Aweeka, PharmD, San Francisco General Hospital, San Francisco, Calif; Beatrice Montelongo, Whitier, Calif; Joan Drucker, MD, Trimeris, Inc, Durham, NC; Frank Duff, MD, and Patricia DeLora, Hoffmann-La Roche Inc, Nutley, NJ.

The PACTG 1005 Study Team and the authors express thanks to the following investigators and site personnel who enrolled patients into this demanding study: Ross McKinney, MD, and Lori Ferguson, Duke University Medical Center, Durham, NC; Andrew Wiznia, MD, and Wanda Biernick, Jacobi Medical Center, New York, NY; Mary Jo Hoyt and Lisa Monti, University of Medicine & Dentistry of New Jersey, Newark, NJ; Kathie Contello, Emily Barr, and Maureen Famliegetti, SUNY Upstate Medical University, Syracuse, NY; So-hail Rana, MD, Helga Finke, and Patricia Wu, Howard University Hospital, Washington, DC; William Borkowsky, MD, M. Sinitzskaya, MD, and Nagamah (Sandra) Deygoo, New York University, New York, NY; John Sullivan, MD, and Donna Christian, University of Massachusetts Medical School, Boston, Mass; and Maryanne Dillon, Childrens Hospital, Los Angeles, Calif.

In the matter of this manuscript, the authors have no financial or personal conflict of interest.

## References

1. Palella FJJ, Delaney KM, Moorman AC, Loveless MO, Fuhrer J, Satten GA, et al. Declining morbidity and mortality among patients with advanced human immunodeficiency virus infection. HIV Outpatient Study Investigators. *N Engl J Med* 1998;338:853-60.
2. Starr SE, Fletcher CV, Spector SA, Yong FH, Fenton T, Brundage RC, et al. Combination therapy with efavirenz,

- nelfinavir, and nucleoside reverse-transcriptase inhibitors in children infected with human immunodeficiency virus type 1. Pediatric AIDS Clinical Trials Group 382 Team. *N Engl J Med* 1999;341:1874-81.
- Murphy EL, Collier AC, Kalish LA, Assmann SF, Para MF, Flanagan TP, et al. Highly active antiretroviral therapy decreases mortality and morbidity in patients with advanced HIV disease. *Ann Intern Med* 2001;135:17-26.
  - Paediatric European Network for Treatment of AIDS (PENTA). Comparison of dual nucleoside-analogue reverse-transcriptase inhibitor regimens with and without nelfinavir in children with HIV-1 who have not previously been treated: the PENTA 5 randomised trial. *Lancet* 2002;359:733-40.
  - De Clercq E. New developments in anti-HIV chemotherapy. *Curr Med Chem* 2001;8:1543-72.
  - LaBranche CC, Galasso G, Moore JP, Bolognesi DP, Hirsch MS, Hammer SM. HIV fusion and its inhibition. *Antiviral Res* 2001;50:95-115.
  - Kliger Y, Peisajovich SG, Blumenthal R, Shai Y. Membrane-induced conformational change during the activation of HIV-1 gp41. *J Mol Biol* 2000;301:905-14.
  - Kilby JM, Eron JJ. Novel therapies based on mechanisms of HIV-1 cell entry. *N Engl J Med* 2003;348:2228-38.
  - Rimsky LT, Shugars DC, Matthews TJ. Determinants of human immunodeficiency virus type 1 resistance to gp41-derived inhibitory peptides. *J Virol* 1998;72:986-93.
  - Jiang S, Zhao Q, Debnath AK. Peptide and non-peptide HIV fusion inhibitors. *Curr Pharm Des* 2002;8:563-80.
  - Lalezari JP, Henry K, O'Hearn M, Montaner J, Piliero P, Trottier B, et al. Enfuvirtide, an HIV-1 fusion inhibitor, for drug-resistant HIV infection in North and South America. *N Engl J Med* 2003;348:2175-85.
  - Lazzarin A, Clotet B, Cooper D, Reynes J, Arasteh K, Nelson M, et al. Efficacy of enfuvirtide in patients infected with drug-resistant HIV-1 in Europe and Australia. *N Engl J Med* 2003;348:2186-95.
  - Moyle G. Finally, the new drug classes arrive. *Curr Opin Infect Dis* 2003;16:1-3.
  - Church JA, Cunningham C, Hughes M, Palumbo P, Mofenson LM, Delora P, et al. Safety and antiretroviral activity of chronic subcutaneous administration of T-20 in human immunodeficiency virus 1-infected children. *Pediatr Infect Dis J* 2002;21:653-9.
  - Kilby JM, Hopkins S, Venetta TM, DiMassimo B, Cloud GA, Lee JY, et al. Potent suppression of HIV-1 replication in humans by T-20, a peptide inhibitor of gp41-mediated virus entry. *Nat Med* 1998;4:1302-7.
  - Lalezari J, Eron JJ, Carlson M, Arduino RC, Goodgame JC, Cohen C, et al. Safety, pharmacokinetics, and antiviral activity of T-20 as a single agent in heavily pretreated patients [abstract LB13]. Presented at the Sixth Conference on Retroviruses and Opportunistic Infections: A Summary on Recent Advances on Antiretroviral Therapy; 1999 Jan 31–Feb 4; Chicago, Ill. Available from: URL: <http://www.thebody.com/confs/retro99/lb13.html>.
  - Kilby JM, Lalezari JP, Eron JJ, Carlson M, Cohen C, Arduino RC, et al. The safety, plasma pharmacokinetics, and antiviral activity of subcutaneous enfuvirtide (T-20), a peptide inhibitor of gp41-mediated virus fusion, in HIV-infected adults. *AIDS Res Hum Retroviruses* 2002;18:685-93.
  - Zhang X, Nieforth K, Lang JM, Rouzier-Panis R, Reynes J, Dorr A, et al. Pharmacokinetics of plasma enfuvirtide after subcutaneous administration to patients with human immunodeficiency virus: inverse Gaussian density absorption and 2-compartment disposition. *Clin Pharmacol Ther* 2002;72:10-9.
  - Bellibas E, Pepper T, Dorr A, Bertasso A, Sista P, Duff F, et al. Pharmacokinetics and safety of 2 mg/kg enfuvirtide (T-20) in combination therapy in HIV-infected children and adolescents [abstract TuPeB4632]. Presented at the Fourteenth International AIDS Conference; 2002 July 7-12; Barcelona, Spain. Available from: URL: [http://www.aids2002.com/Program/ViewAbstract.asp?id=/TCMS\\_Content/Abstract/200206290751164542.xml](http://www.aids2002.com/Program/ViewAbstract.asp?id=/TCMS_Content/Abstract/200206290751164542.xml).
  - Fletcher CV. Enfuvirtide, a new drug for HIV infection. *Lancet* 2003;361:1577-78.
  - Kosel B, Church J, Cunningham C, Sista P, Aweeka F, PACTG P1005 Study Team. Pharmacokinetics (PK) of selected doses of T-20, a fusion inhibitor, in HIV-1 infected children [abstract 726]. Presented at the Eighth Conference on Retroviruses and Opportunistic Infections; 2001 Feb 4-8; Chicago, Ill. Available from: URL: <http://www.retroconference.org/2001/abstracts/abstracts/abstracts/726.htm>. Accessed Oct 28, 2003.
  - Beal SL, Sheiner LB. *NONMEM users guides*. San Francisco (CA): University of California at San Francisco; 1992.
  - Perelson AS, Neumann AU, Markowitz M, Leonard JM, Ho DD. HIV-1 dynamics in vivo: virion clearance rate, infected cell life-span, and viral generation time. *Science* 1996;271:1582-6.
  - Bonhoeffer S, May R, Shaw G, Nowak M. Virus dynamics and drug therapy. *Proc Natl Acad Sci U S A* 1997;94:6971-6.
  - Ogg G, Jin X, Bonhoeffer S, Moss P, Nowak A, Monard S, et al. Decay kinetics of human immunodeficiency virus-specific effector cytotoxic T lymphocytes after combination antiretroviral therapy. *J Virol* 1999;73:797-800.
  - Nelson PW, Mittler JE, Perelson AS. Effect of drug efficacy and the eclipse phase of the viral life cycle on estimates of HIV viral dynamic parameters. *J Acquir Immune Defic Syndr* 2001;26:405-12.
  - Wu H, Wu L. Identification of significant host factors for HIV dynamics modelled by non-linear mixed-effects models. *Stat Med* 2002;21:753-71.
  - Kaul S, Kline MW, Church JA, Dunkle LM. Determination of dosing guidelines for stavudine (2',3'-didehydro-3'-deoxythymidine) in children with human immunodeficiency virus infection. *Antimicrob Agents Chemother* 2001;45:758-63.

29. Capparelli EV, Sullivan JL, Mofenson L, Smith E, Graham B, Britto P, et al. Pharmacokinetics of nelfinavir in human immunodeficiency virus-infected infants. *Pediatr Infect Dis J* 2001;20:746-51.
30. Grub S, Delora P, Ludin E, Duff F, Fletcher CV, Brundage RC, et al. Pharmacokinetics and pharmacodynamics of saquinavir in pediatric patients with human immunodeficiency virus infection. *Clin Pharmacol Ther* 2002;71:122-30.
31. Zhang X, Patel IH, Lalezari J, Badley A, Hawker N, Dorr A, et al. Assessment of metabolic inhibition potential of enfuvirtide using a 5-drug cocktail in HIV-1 infected patients [abstract PIII-73]. *Clin Pharmacol Ther* 2003;73:P81.
32. Kovarik JM, Offner G, Broyer M, Niaudet P, Loirat C, Mentser M, et al. A rational dosing algorithm for basiliximab (Simulect) in pediatric renal transplantation based on pharmacokinetic-dynamic evaluations. *Transplantation* 2002;74:966-71.
33. Wheat L, Lalezari JP, Kilby M, Wheeler D, Salgo M, DeMasi R, et al. A week-48 assessment of high strength T-20 formulations in multi-class experienced patients [abstract 417-W]. Presented at the Ninth Conference on Retroviruses and Opportunistic Infections; 2002 Feb 24-28; Seattle, Wash. Available from: URL: <http://www.ret-roconference.org/2002/Abstract/13553.htm>.

## APPENDIX

**Population pharmacokinetic model.** The state (amounts in compartments) of a pharmacokinetic (PK) model for a generic individual at time  $t$  is given by the solution to the following system of differential equations (1-compartment PK model with extravascular administration):

$$\frac{dA_0(t)}{dt} = -k_a A_0$$

$$\frac{dA_1(t)}{dt} = k_a A_0 - \frac{CL}{V} A_1$$

in which  $A_0$  and  $A_1$  are the amounts of drug in the subcutaneous absorption site and the central compartment, respectively;  $k_a$  is the absorption rate constant from the absorption compartment;  $CL$  is the total clearance from the central compartment; and  $V$  is the volume of that compartment. Initial conditions for a bolus intravenous dose are as follows:  $A_1(0) = D$ , in which  $D$  is dose amount, and  $A_0(0) = 0$ . For a subcutaneous bolus dose experiment,  $A_0(0) = F \cdot D$ , in which  $F$  is bioavailability. Standard formulas<sup>1</sup> yield the initial conditions for steady-state subcutaneous dosing.

The observation (concentration) at time  $t$  is given by the following equation:

$$C(t) = \frac{A_1(t)}{V} + \epsilon(t)$$

in which  $\epsilon(t)$  is a normally distributed random error, independent of errors at other times, with variance equal to  $\sigma^2[1 + \theta_{SP,3}SP(t)]$ , in which  $\theta_{SP,3}$  is a param-

eter and  $SP(t)$  takes the value of 1 if the observation at time  $t$  is a "sparse sample" and 0 otherwise.

For a generic PK parameter,  $P$  (ie, either  $CL$ ,  $V$ ,  $F$ , or  $k_a$ ), the following model is used:

$$P = \mu_P \exp(\eta_P)$$

in which  $\mu_P$  is the population mean of  $P$  and  $\eta_P$  is a normally distributed random effect [ $N \sim (0, \omega_P^2)$ ], capturing the interindividual variability of  $P$ . The random effects for different parameters may be correlated.

A mean parameter  $\mu_P$  may be further modeled as a function of covariates, for example:

$$\mu_P = \theta_{P,1} WT^{\theta_{P,2}}$$

or

$$\mu_P(t) = \theta_{P,1}[(1 - SP) + \theta_{P,3}SP]$$

in which  $\theta_{P,k}$  ( $k = 1, 2, 3$ ) represents elements of a vector of population fixed effect parameters and  $WT$  is patient weight; the second example makes the point (because  $SP$  changes with time) that population mean parameters may be time-dependent.

**Population pharmacodynamic model.** The state of the viral pharmacodynamic (PD) model for a generic individual at time  $t$  is defined by the solution to the following differential equation (1-compartment model of viral count with zero-order production):

$$\frac{dA_v(t)}{dt} = R \cdot I(t < \tau) - \frac{CL_v}{V_v} \cdot A_v(t)$$

in which  $A_v(t)$  is the number of human immunodeficiency virus ribonucleic acid (RNA) copies in the central compartment at time  $t$ ,  $R$  is the rate of virus production from cells infected before drug administration (viral RNA amount per time) and is to be estimated in the model,  $I$  is the indicator function taking the value 1 if its argument is true and 0 otherwise,  $\tau$  is the persistence time of preinfected cells before releasing viral RNA,  $CL_v$  is the clearance of the virus, and  $V_v$  is the viral volume of distribution. The initial condition at the time of starting treatment is  $A_v(0) = A_{v,0}$ , the baseline viral RNA (amount in the body), and is a parameter to be estimated.

The measured viral RNA concentration  $C_v(t)$  at time  $t$  is given as follows:

$$C_v(t) = \frac{A_v(t)}{V_v} + \epsilon_v(t)$$

in which  $\epsilon_v(t)$  is a residual error, assumed to be distributed as  $N(0, \sigma_v^2)$ .

The PD parameters to be estimated [ $CL_v$ ,  $R$ ,  $\tau$ ,  $A_v(0)$ ] are modeled just as the PK parameters (see earlier), but no covariates are used. Because a known quantity of exogenous virus is never given,  $V_v$  is unidentifiable and it is, therefore, fixed to unity.

## Reference

1. Gibaldi M, Perrier D. *Pharmacokinetics*. Marcel Dekker; 1982. p. 33-9.